PRAMANA
— journal of
physics

© Indian Academy of Sciences

Vol. 71, No. 1
July 2008
pp. 65–75

Full wave analysis of non-radiative dielectric waveguide modulator for the determination of electrical equivalent circuit

N P PATHAK[1,*], A BASU[2] and S K KOUL[2]
[1]Department of Electronics and Computer Engineering, Indian Institute of Technology Roorkee, Roorkee 247 667, India
[2]Centre for Applied Research in Electronics, Indian Institute of Technology Delhi, New Delhi 110 016, India
[*]Corresponding author
E-mail: nagppfec@iitr.ernet.in; ananjan@care.iitd.ernet.in; skkoul@care.iitd.ernet.in

MS received 16 August 2007; accepted 30 January 2008

Abstract. This paper reports the determination of electrical equivalent circuit of ON/OFF modulator in non-radiative dielectric (NRD) guide configurations at Ka-band. Schottky barrier mixer diode is used to realize this modulator and its characteristics are determined experimentally using vector network analyzer. Full wave FEM simulator HFSS is used to determine an equivalent circuit for the mounted diode and modulator in ON and OFF states. This equivalent circuit is used to qualitatively explain the experimental characteristics of modulator.

Keywords. Dielectric waveguide; non-radiative dielectric guide; modulator; millimeter-wave integrated circuits; FEM; Schottky barrier diode.

PACS Nos 41.20.-q; 07.57.-c; 42.79.Gn; 07.50.Ek

1. Introduction

The millimeter-wave region of the electromagnetic spectrum, which typically spans from 30 to 300 GHz, represents a vast spectrum resource with enormous potential applications. Due to smaller wavelengths, greater bandwidth and more interaction with atmospheric constituents, millimeter-wave region is useful in applications requiring high-speed data transmission, broadband cellular communications, secure communications, and a variety of radar systems. The millimeter-wave systems used in the above applications are made of many electronic parts called 'circuits' or 'components'. The technology for the development of these electronic circuits in the microwave frequency range is well developed. Considerable research work is currently being carried out to improve technology for the development of these components in the millimeter-wave frequency region. The main emphasis is to make the

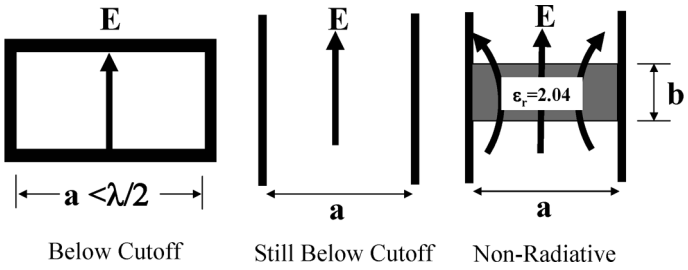


Figure 1. Concept of non-radiative dielectric waveguide.

components more compact, and cost-effective. Non-radiative dielectric waveguide is a prominent transmission medium that can be used to develop high performance and low cost systems at millimeter-wave frequencies [1–3]. NRD guide consists of a rectangular dielectric strip, of cross-section $a \times b$ and relative dielectric constant ε_r, which is sandwiched between two parallel metal ground plates (figure 1). The plate separation a is less than half the free-space wavelength ($\lambda_0/2$) so that fields are cut off in the air region. The presence of dielectric strip enables electromagnetic waves to propagate along the strip, whereas, radiated waves due to discontinuities in the structure are suppressed because of the cut-off nature of the surrounding air-filled region. The incident field should exhibit symmetry giving a perfect magnetic conductor (PMC) midway between the metal plates. This waveguide structure supports two modes that are non-radiative (figure 2). The first non-radiative mode is the LSE_{11} mode and the second non-radiative mode is the LSM_{11} mode. Since the E-field lines for the LSE_{11} mode are mainly perpendicular to the NRD guide ground planes, it is a lossy parasitic mode and is undesirable. The E-field lines for LSM_{11} mode are mainly parallel to the ground metal plates; hence it is a low loss mode used in the design of NRD guide circuits. The NRD guide excited in the low loss LSM_{11} mode serves as the basic building block for developing various transceiver circuit elements at millimeter-wave frequencies. In certain cases, a mode suppresser is used to suppress the undesired LSE_{11} mode. The NRD guide structure also supports several parallel-plate types of modes, with E-field lines originating from one plate and terminating on the other. To avoid these modes, NRD guide components are usually made symmetrical about the plane parallel to and midway between the ground planes. If the feed (usually rectangular waveguide) also conforms to this symmetry (the symmetry plane effectively becomes a perfect magnetic conductor (PMC), then only the LSE_{11} and LSM_{11} modes can propagate. Dispersion characteristics of NRD guide is shown in figure 3.

2. NRD guide ON/OFF modulator

The lay-out of the ON/OFF modulator circuit that is implemented in NRD guide configuration [4,5] is shown in figure 4. As seen from the figure, input/output transmission lines are implemented by straight sections of NRD guide strip made of teflon ($\varepsilon_r = 2.04$) that is linearly tapered at the ends for feeding power from the

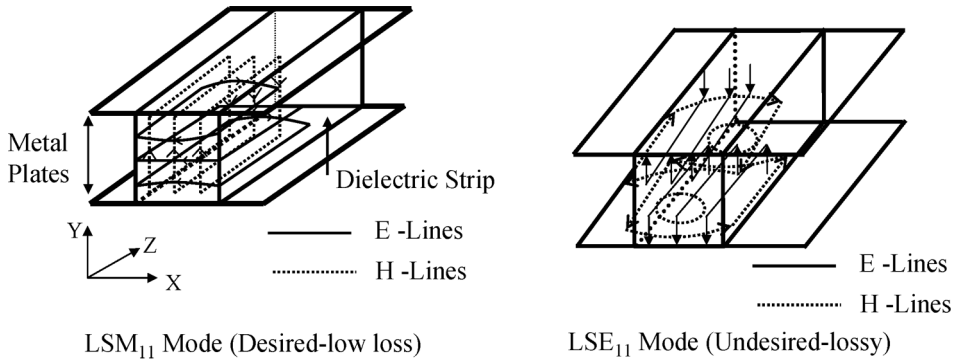


Figure 2. Propagating modes in NRD guide.

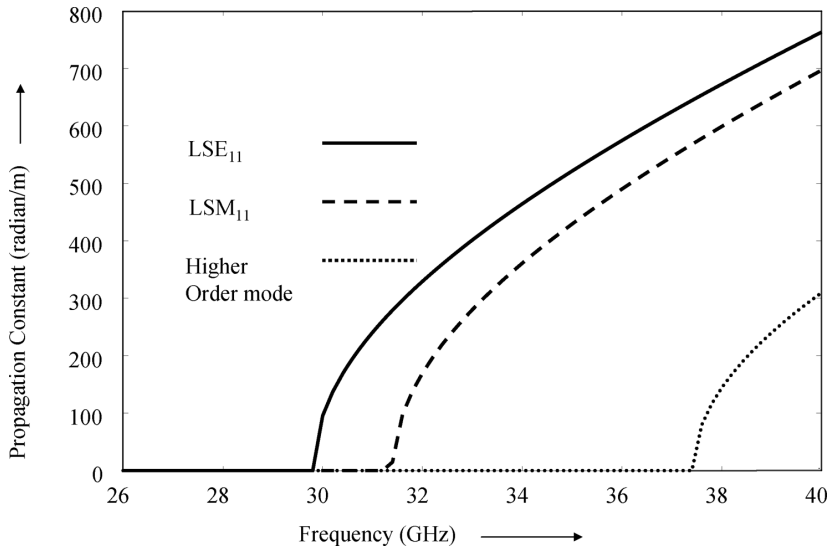


Figure 3. Dispersion characteristics of NRD guide.

rectangular waveguide. The cross-section of teflon strip is 4 mm × 4 mm that is based on the criteria given in eq. (1).

$$\frac{a}{\lambda_0} \approx 0.45, \qquad \frac{b}{\lambda_0}\sqrt{\varepsilon_r - 1} \approx 0.4\text{–}0.6. \tag{1}$$

2.1 *Matching network for modulator*

It is important to design a suitable matching network to minimize reflection loss. The circuit used for impedance matching of the diode comprises an air gap (g) and a piece of teflon strip (ℓ_r) (figure 5a). Full wave simulation is carried out to

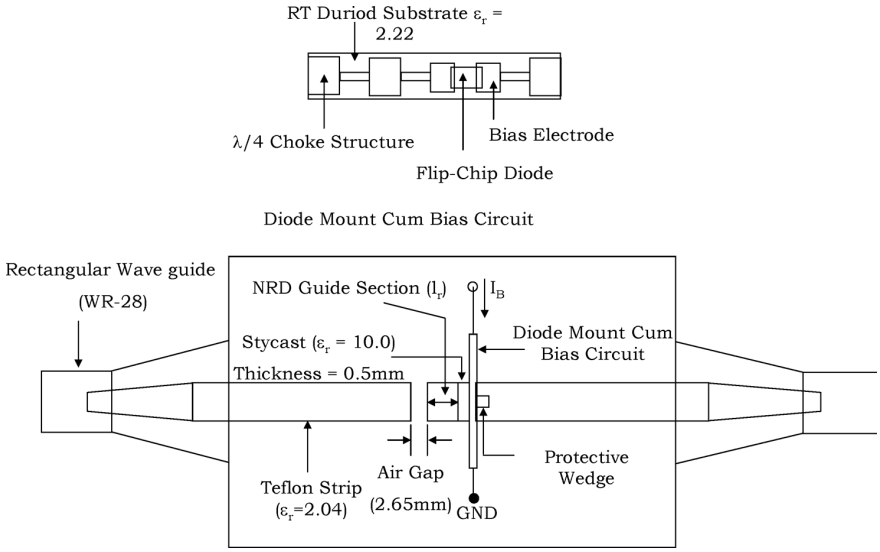


Figure 4. Lay-out of NRD guide ON/OFF modulator.

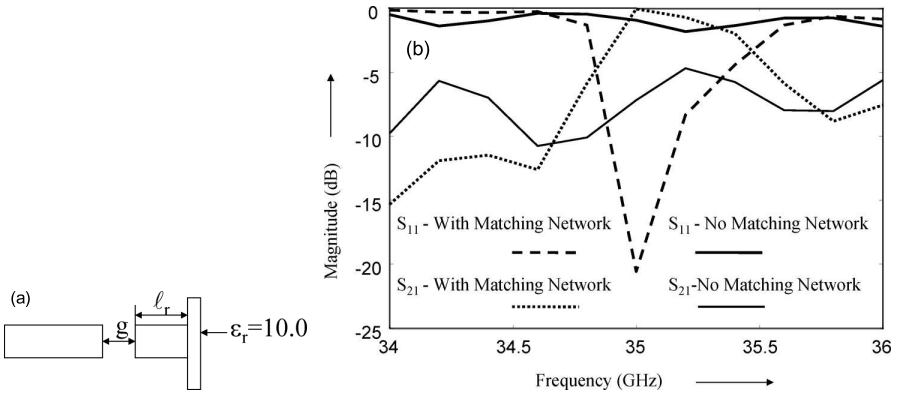


Figure 5. (**a**) Matching network used in the development of modulator. (**b**) Effect of diode matching on the modulator characteristics.

show the necessity of diode matching network. As seen from figure 4, the matching network is placed at the RF input side. In the absence of matching network, the input and output connection to the diode is provided by straight section of teflon strips. Figure 5 shows the simulated response of modulator with and without diode-matching network. As expected, the diode-matching network improves the transmission coefficient considerably over a narrow band. It is, therefore, necessary to incorporate a suitable diode-matching network so that power can be transferred from the input port to the output port with minimum reflection from the diode at the desired frequency. By changing ℓ_r, the operating frequency of the modulator is changed. The variation of modulator output as a function of length ℓ_r of teflon strip used for matching is given in figure 6. The optimized dimensions of the air

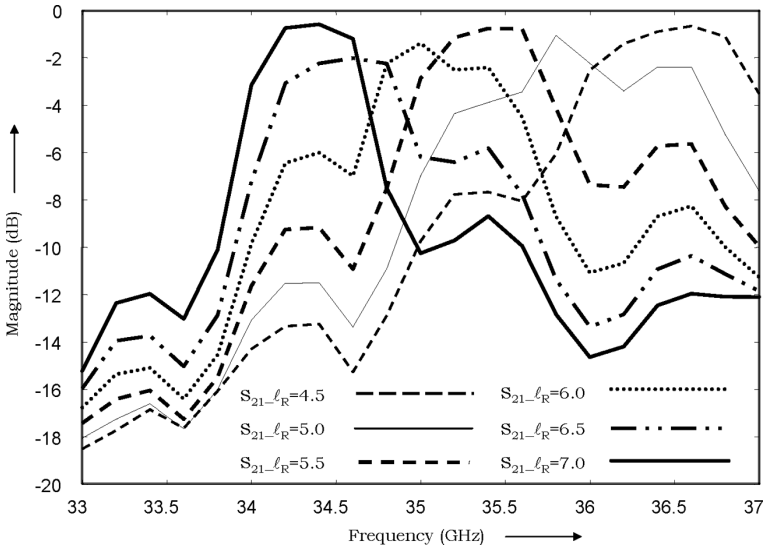


Figure 6. Variation of modulator output as a function of resonator length.

gap is 2.65 mm and the length of teflon strip used for matching is $\ell_r = 5.5$ mm. To improve matching, a high dielectric constant strip made of Stycast ($\varepsilon_r = 10.2$) of thickness 0.5 mm is placed in front of the diode. On the other side of the diode, a wedge is created in the output teflon strip to protect the diode from damage. In order to keep the losses low, it is necessary that the teflon strips make perfect contact with the ground planes without any air gap. Applying slight pressure to the NRD guide ground plates or using a low loss adhesive can achieve this.

2.2 *Diode mount cum bias choke circuit*

One of the most critical parts in the modulator is the circuit that enables the coupling of electromagnetic energy from dielectric strip to Schottky barrier diode. Since diode can only be fixed onto the metal surface, planar transmission line geometry is used as the diode mount. Stripline like circuit is found to be most suitable for this purpose. The bias choke structure is a low pass filter type structure that acts as a band reject filter at the design frequency, i.e. the frequency at which the electrical length of the elements is 90°. This same mounting technique is suggested in [4,5] and hence used in the development of the present modulator. The diode mount cum bias choke consists of a $\lambda/4$ choke structure with mounting pads for the diode. This pattern prevents the generation of TEM stripline modes. The $\lambda/4$ choke pattern is etched out by photolithography technique on 10-mil RT-duroid substrate ($\varepsilon_r = 2.22$). The ground metallization is removed, since a stripline-like structure (here metallization plane is perpendicular to ground planes) is used. The gap left for diode bonding is 0.3 mm as suggested in the manufacturer's catalog [6]. The flip chip Schottky barrier diode from Alpha Industries (DMK2790) is bonded

using flexible conductive epoxy and is cured at 100°C for 1 h. Since the available epoxy is not a standard product, its use increases losses that are difficult to predict. The bias voltage is directly applied to the modulator by connecting a DC supply and using a suitable resistance (470 Ω in this case) at one end of the choke and grounding the negative end of the diode.

2.3 *Modulator characteristics*

After the preparation of individual components of the modulator, such as tapered NRD guide sections for the input and output, dielectric strip for matching network, high dielectric constant sheet and a wedged section of dielectric strip, diode is mounted on photoetched $\lambda/4$ bias choke structure and the modulator is assembled in its final form as shown in figure 4. To measure the characteristics of the fabricated modulator, we have used vector network analyzer (VNA) of Rhode and Schwarz make (model ZVK). A DC power supply is used to provide bias to the diode. The input/output coaxial cables of VNA are connected to the standard rectangular waveguide (WR-28). A tapered horn antenna (in E- and H-planes) is used as a transition from rectangular waveguide to NRD guide. The dielectric strip of input and output NRD guide section is tapered in E- and H-planes to provide smooth field matching. The development of NRD guide to WR-28 rectangular waveguide transition is given in [7]. The measured characteristics of back-to-back NRD guide to WR-28 transition, which is used in the measurement of modulator characteristics, is shown in figure 7. After connecting the cables properly, bias is applied to the diode. The measured S-parameters of modulator in the ON- and OFF-states are shown in figure 8. Inspection of the modulator or switch characteristics reveals that the output (S_{21}) is high when diode is biased (ON-state) and the output is low when diode is unbiased (OFF-state). Since, for the dominant LSM_{11} mode of the NRD guide, E-field lines are parallel to metal plates it is expected that in the ON-state, diode should reflect all the power and output should be low; while in the OFF-state of the diode, no reflection should take place and hence output should be high.

3. Equivalent circuit of diode and modulator

The analysis of NRD guide modulator was reported in [4,8,9]. Full wave analysis reported in [4] uses FEM [10] in conjunction with circuit simulator [11] to obtain the modulator characteristics. In all these reported works there is no description about the equivalent circuit of mounted diode and modulator. In order to explain the modulator characteristics, it is essential to obtain the equivalent circuit of the diode and the modulator for ON- and OFF-states. It is observed from the diode geometry that there are conducting metal pads on GaAs substrate in addition to the active diode region. To find out the electrical equivalent circuit of the diode chip, FEM technique is applied. To simplify the problem, diode is mounted in shunt with 50 Ω-microstripline as shown in figure 9a. In the first configuration, positive end of the diode is connected to a 50 Ω line in the microstrip, while negative end is

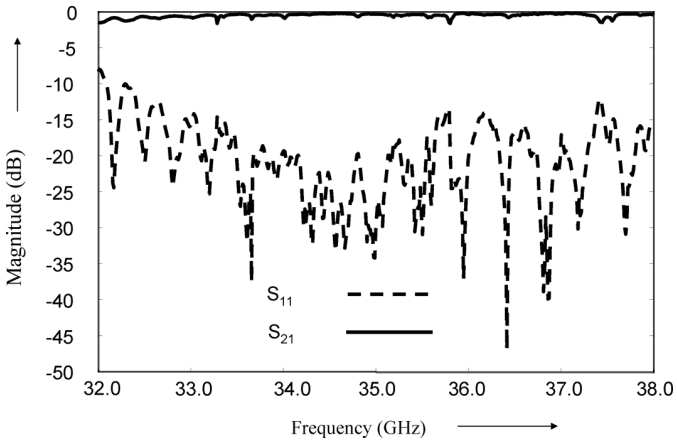


Figure 7. Measured characteristics of NRD guide to WR-28 back-to-back transition.

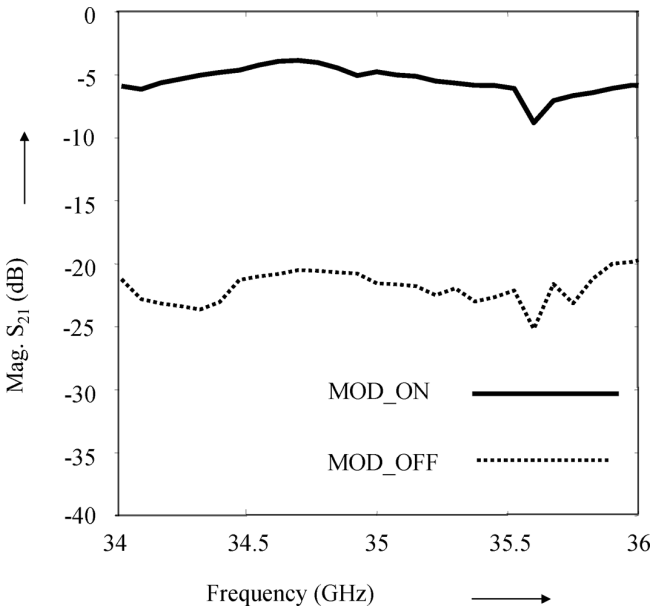


Figure 8. Measured characteristics of the modulator circuit.

grounded. In this case, presence of the microstrip ground plane completely alters the field pattern near the diode.

In the second configuration, the diode is oriented vertically in a fully shielded microstrip line having very small channel dimensions. The positive end of the diode remains connected to the 50 Ω line, but the negative end gets connected to the upper ground plane. This structure can be easily and accurately analysed using HFSS. The second configuration is similar to the practical situation in the

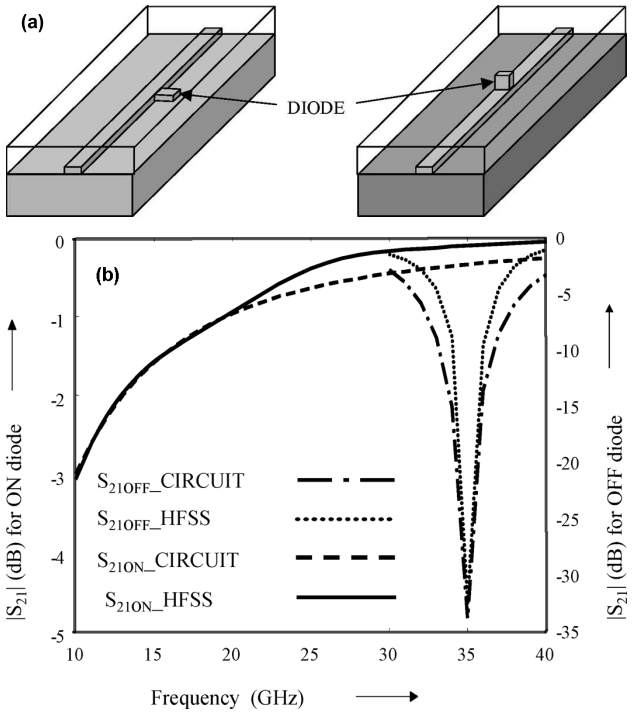


Figure 9. (**a**) Two possible techniques of shunt mounting the diode. (**b**) Comparison of simulated results obtained using FEM with those obtained using the lumped equivalent circuit models.

NRD guide and hence it is used to obtain the equivalent circuit. Connecting the active diode area by perfect metal strip or leaving a gap in between, respectively, implement the ON- and OFF-states of the diode in the ideal case. Figure 9b shows the simulated S_{21} for the ON- and OFF-states. The circuit simulator is now used to match the simulated results of the diode in the ON- and OFF-states. The lumped element equivalent circuit of the diode in the ON-state is a series inductor of 0.4 nH. In the OFF-state, the lumped element equivalent circuit is a series LC (0.4 nH inductor in series with 52 fF capacitor) circuit connected in shunt to the main line. The expressions for the S_{21} of the lumped circuits in the ON- and OFF-states are given by (2) and (3), respectively.

$$S_{21}(\mathrm{ON}) = \frac{j2\omega L}{50 + j2\omega L}, \tag{2}$$

$$S_{21}(\mathrm{OFF}) = \frac{2(\omega^2 LC - 1)}{2\left(\omega^2 LC - 1\right) - j50\omega C}. \tag{3}$$

Figure 9b shows comparison of simulated results obtained using FEM with those obtained using the lumped equivalent circuit models. As observed, the response of lumped equivalent circuit matches closely with the results obtained using full wave

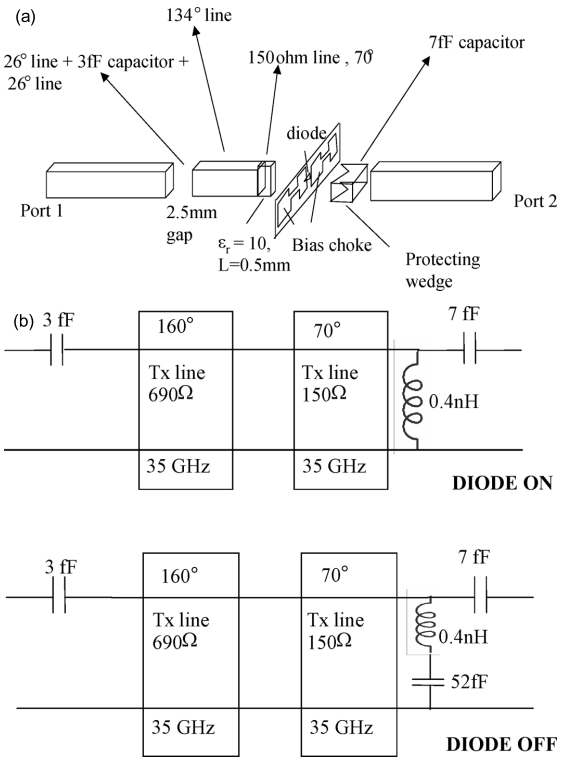


Figure 10. (**a**) Various parts of the modulator. (**b**) Transmission line equivalent circuits of the modulator in ON- and OFF-states.

analysis (including phase, which is not shown here). This clearly indicates that the derived lumped equivalent circuit models of the diode for the ON- and OFF-states are reasonably accurate. The problem of determining the transmission line-based equivalent circuit for the entire modulator circuit was taken up next. Details of a typical modulator circuit are described in [3,4]. Figure 10 a shows different parts of the modulator along with their equivalent circuits. In the following, justification for these equivalent circuits is presented:

(a) The gap in the NRD guide (2.5 mm) at 35 GHz gives simulated S_{21} of $0.68\angle{-5}°$, while a series capacitor of 3 fF gives S_{21} of $0.68\angle 47°$. Therefore, the equivalent circuit should be a 3 fF series capacitor, with transmission lines of 26° electrical lengths on either side to adjust the phase. One of these lines can be absorbed in port 1; the other needs to be added to the transmission line that is the next element.

(b) A uniform section of 5.5 mm long NRD guide is 134° at 35 GHz. Additional electrical length of 26° from the preceding capacitor is added to give total electrical length of 160°.

(c) A sheet of high dielectric constant ($\varepsilon_r = 10$) gives a simulated $S_{21} = 0.46\angle{-80}°$ at 35 GHz. This is modeled by a 150 Ω transmission line of electrical length 70°, which has $S_{21} = 0.44\angle{-81}°$.

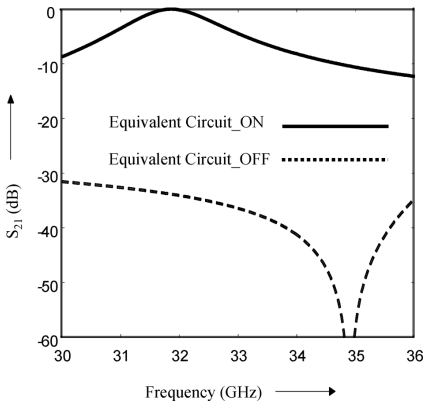


Figure 11. Response of the modulator using transmission line equivalent circuit shown in figure 10b.

(d) Depending on the bias state, the diode is replaced by its L or LC equivalent circuit. The bias choke on which the diode is mounted is neglected, since there is no simple equivalent circuit for this 3D structure. This is expected to affect the results substantially.

(e) The protective wedge (air partially replacing the teflon) in the final NRD guide connecting to port 2 is modeled as a 7 fF capacitor. This value is somewhat arbitrary. However, the circuit performance is only weakly dependant on this parameter.

The equivalent circuit of NRD guide modulator is shown in figure 10b. The port reference has been taken as 690 Ω, this being the 'power-voltage' impedance of the NRD guide under consideration. The value of port impedance is not particularly important, since all the values above are derived from S-parameters that can be scaled to any impedance. The simulated response of the modulator using the ideal transmission line equivalent circuit shown in figure 10b is plotted in figure 11. A considerable frequency shift in centre frequency from 35 GHz to 32 GHz with a narrow pass-band is observed for the ON-state. This characteristic differs from the one obtained experimentally and also using full-wave simulation. However, the essential switching behavior is observed. The simulated performance of the modulator using simplified transmission line equivalent circuit qualitatively explains the experimentally observed behavior of the modulator that has also been reported in [5]. For quantitative results full-wave simulation is required.

4. Conclusions

Full wave analysis using finite element method has been used to develop an electrical equivalent circuit of mounted Schottky barrier diode. The equivalent circuit is derived from the measured data and circuit/electromagnetic simulation method by mounting the diode in shunt with the 50 Ω microstripline. The equivalent circuit model of the diode for the ON- and OFF-states when used with the ideal

transmission line equivalent circuit of the modulator gives similar response as observed from measurements and rigorous full wave analysis of the modulator.

References

[1] T Yoneyama and S Nishida, *IEEE Trans. on Microwave Theory and Techniques* **MTT-29(11)**, 1188 (1981)
[2] F Kuroki, M Sugioka, S Matsukawa, K Ikeda and T Yoneyama, *IEEE Trans. on Microwave Theory and Techniques* **46(6)**, 806 (1998)
[3] S K Koul, *Millimeter wave and optical dielectric integrated guides and circuits* (John Wiley & Sons, Inc., New York, 1997)
[4] T Yoneyama, *IEEE MTT-S Int. Microwave Symposium Dig.* (1989) pp. 1083–1086
[5] N P Pathak, A Basu, S K Koul and B Bhat, *IEEE Microwave and Wireless Components Letters* **14(7)**, 322 (2004)
[6] *Discrete semiconductor devices for RF/microwave applications* (Alpha, Woburn, MA, 2000) pp. 3.24–3.27
[7] J A G Malherbe, J H Cloete and I E Losch, *IEEE Trans. on Microwave Theory and Techniques* **MTT-33(6)**, 539 (1985)
[8] W A A Junior, *Proc of SBMO/IEEE MTT-S Int. Microwaves and Optoelectronics Conference* (IMOC97), 1997, pp. 344–349
[9] F Kuroki, S Shinke and T Yoneyama, *Proc. of 11th IEEE International Symposium on Electron Devices for Microwave and Optoelectronics Applications* (EDMO2003), 2003, pp. 229–233
[10] HFSS 5.5 User's guide (Agilent Technologies, Palo Alto, CA, 2000) pp. 11.2–11.20
[11] Agilent Advanced Design System 2003A User Manual (Agilent Technologies, Palo Alto, CA, 2003)